Chaotic self-trapped optical beams in strongly nonlocal nonlinear media

Lanhua Zhong,[1] Qi Guo,[2,*] Wei Hu,[2] Weiyi Hong,[2] and Wei Xie[1]
[1]*Physical Science and Technology School, Lingnan Normal University, Zhanjiang 524048, China*
[2]*Guangdong Provincial Key Laboratory of Nanophotonic Functional Materials and Devices, South China Normal University, Guangzhou 510631, China*

(Received 6 January 2019; revised manuscript received 22 February 2019; published 15 April 2019)

The self-trapped optical beams possessing both chaotic and solitonlike properties, which are termed as chaoticons, were predicted by us [Sci. Rep. **7**, 41438 (2017)] in the strongly nonlocal nonlinear media. We reveal that any random input beam, which has random initial transverse distribution and arbitrary input power, propagating in the strongly nonlocal nonlinear media with the exponential-decay response, will evolve into a chaoticon. The chaotic properties are signified by the positive Lyapunov exponents and spatial decoherence, while the solitonlike properties are demonstrated by the invariance of the beam width and the interaction of quasielastic collisions. Distinctively, the propagations of random inputs are always periodic in the strongly nonlocal media with the Gaussian response.

DOI: 10.1103/PhysRevA.99.043816

I. INTRODUCTION

An important class of nonlinearities in optics is associated with the nonlocal process, the mechanism of which includes the molecular reorientation, the thermal nonlinearity, the photorefractive effect, the electrostriction, etc. Nonlocal nonlinearity means that the nonlinear response at a certain spatial point is determined not only by the optical wave at that point but also by the wave in its vicinity; the stronger the nonlocality, the larger range of wave concerned [1–3]. Since the pioneering theoretical work in 1997 [3], in which the nonlinear equation guiding the paraxial propagation of beams under the condition of strong nonlocality was simplified to a linear model and the nonlocal spatial solitons were predicted, experimenters have discovered several media with strong nonlocality. The most extensively studied ones are the nematic liquid crystals [4–10] and the lead glass [11–18]. In the strongly nonlocal nonlinear media, some interesting phenomena have been found, such as it supports various types of complex spatial solitons [7,11–13,19,20].

The nonlocal nonlinearity can be described by the nonlinear response function, which is usually of different form in different kinds of media. For instance, there is the logarithmic response function in the lead-glass [15–18], the exponential-decay response function (ERF) in the (positive) nematic liquid crystals [1,2,7–9,20,21], the sine-oscillatory response function in the negative nematic liquid crystals [22,23], and so on. In addition, the rather unphysical but extremely instructive Gaussian response function (GRF) has been considered abundantly owing to the convenience of an analytical treatment [7,19,21,24–27]. The response function plays an important role in the behavior of beams propagating in the media. For the (1+1)-dimensional Kerr-type nonlocal nonlinear system, in both cases with GRF and ERF there exist the Hermitian-Gaussian-type stationary solutions (HGSS) [8,26]: $q(x,z) = u_N(x)\exp(ib_N z)$, where $q(x,z)$ is the dimensionless slowly varying complex amplitude of the optical field, x and z stand for the transverse and propagation directions, respectively, the transverse profile function $u_N(x)$ is of the Hermitian-Gaussian-like shape with N ($N \geqslant 1$) humps, b_N is a real constant, $P_N = \int_{-\infty}^{\infty} |u_N(x)|^2 dx$ is the critical power of the HGSS. However, the stability of the HGSS are different. In the GRF system, all of the HGSS are stable and form spatial solitons [7,26]. While in the ERF system, only the low-order HGSS (with $N < 5$) are stable [7], the high-order ones (with $N \geqslant 5$) are unstable, which will evolve into chaoticons (chaotic solutions meanwhile exhibit solitonlike properties) under the condition of strong nonlocality [9]. Chaoticons, as a new kind of beams occurring in the strongly nonlocal nonlinear media [9], whose model is different from the chaoticons of the dissipative system [28,29], have been largely unexploited to the best of our knowledge.

On the other hand, the model describing the propagation of beams in a nonlocal nonlinear media, expressing as the nonlocal nonlinear Schrödinger equation, is a nonintegrable conservative system. It is well known that, for a conservative nonlinear system, the existence of chaos depends not only on the equation and the parameters therein, but also on the initial values [30–32]. Then an open question is whether the chaos takes place only under the initial conditions of $q(x,0) = u_N(x)$, or it happens generally. Or in other words, will an initial input other than the high-order HGSS evolve into a chaoticon? Our aim of this work is to answer the question by studying numerically the evolutions of random initial inputs in the strongly nonlocal nonlinear media.

The paper is organized as follows. In Sec. II, we simulate the propagation of random initial inputs in the ERF and the GRF systems. For a clear comparison with the initial inputs of the HGSS, we first select a random initial input with the same power and beam width as the HGSS, and then change the initial power to make the initial input stand for a

*Corresponding author: guoq@scnu.edu.cn

completely random input. In Sec. III, the maximal Lyapunov exponents and the spatial cross correlation function during the propagation are computed. In Sec. IV, the interaction of two equivalent beams are simulated. Section V presents our conclusion that chaoticons exist generally in the strongly nonlocal nonlinear media with the ERF.

II. EVOLUTIONS OF RANDOM INITIAL INPUTS

The paraxial propagation of a (1+1)-dimensional light beam in media with a Kerr-type nonlocal nonlinearity is governed by the nonlocal nonlinear Schrödinger equation [1,2]

$$i\frac{\partial q}{\partial z}+\frac{1}{2}\frac{\partial^2 q}{\partial x^2}+q\int_{-\infty}^{\infty}R(x-\xi)|q(\xi,z)|^2d\xi=0, \quad (1)$$

where $R(x)$ is the normalized $[\int_{-\infty}^{\infty}R(x)dx=1]$ nonlinear response function. It contains both the effects of diffractive spreading [depending on the profile of $q(x)$] and nonlinear self-focusing (depending on the power of the beam in strong nonlocality), which are commensurable in our scope of discussion. We consider here the ERF, which is also referred to as the diffusive type of nonlinearity [20],

$$R(x)=\frac{1}{2w_m}\exp(-\frac{|x|}{w_m}), \quad (2)$$

where w_m is the characteristic length of the response function. In general, a strong nonlocality means the ratio $w/w_m\leqslant 0.1$, in which the beam width w is defined statistically by the second-order moment [8,9,22,26]

$$w(z)=\sqrt{\frac{2}{P}\int_{-\infty}^{\infty}[x-x_c(z)]^2|q(x,z)|^2dx}, \quad (3)$$

where $x_c(z)=\int_{-\infty}^{\infty}x|q(x,z)|^2dx/P$ is the center of the beam, $P=\int_{-\infty}^{\infty}|q(x,z)|^2dx$ is the power of the beam. In the spectrum space, the statistic beam width can be calculated in the same way as Eq. (3) via firstly obtaining the Fourier spectrum $\tilde{q}(k,z)=\int q(x,z)\exp(-ikx)dx$.

In order to find out the dependence of the existence of chaoticons on the initial value, we change the initial value from the HGSS step by step. In the (1+1)-dimensional dimensionless system, a normal-incidence beam can be characterized by three parameters: the transverse profile, the power and the beam width. First, we change the transverse profile and keep the other two. That is, we select an initial input with a random profile but holding the same power and statistic beam width with the HGSS in both real space and spectrum space. This kind of inputs can be obtained within two steps: we can always pick out a random profile with a given beam width (both in real and spectrum space) by repeatedly generating random arrays, then we multiply a proper coefficient to make the initial power $P_i=P_N$. An example is shown in Fig. 1(a), in which the solid blue curve denotes a random input $r(x)$ with the beam width and power equivalent to the nine-humped HGSS [the black dotted curve in Fig. 1(a)]. The evolution of the initial input $q(x,0)=r(x)$ under the condition of strong nonlocality [$w_m=10$ and $w(0)=1$ unless otherwise stated] is shown in Figs. 1(b)–1(e), including the contour plots of the amplitude $|q(x,z)|$ (instead of the intensity $|q(x,z)|^2$ for a better discernibility) in Figs. 1(b) and 1(c) and the statistic

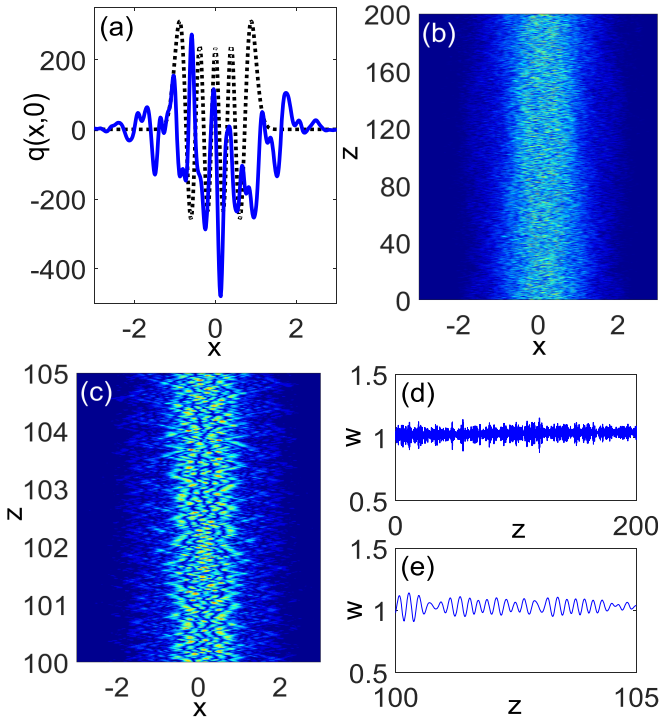

FIG. 1. The evolution of a random initial input with $P_i=P_9$ in the ERF model. (a) The initial input $r(x)$ (blue solid curve) with a random profile holding the same power and beam width with the nine-humped HGSS (black dotted curve). (b), (c) The contour plots of $|q(x,z)|$, (d), (e) the corresponding statistic beam widths $w(z)$. (c), (e)The enlargements of (b), (d) in the region of $z\in[100,105]$, respectively.

beam width $w(z)$ in Figs. 1(d) and 1(e). Figures 1(c) and 1(e) are the enlargements of 1(b) and 1(d) in the region of $z\in[100,105]$, respectively. It is obvious that the evolutions are aperiodic and irregular. However, the beam width remain roughly invariant, the relative standard deviation of which is less than 4%. The invariance of beam width may be concerned with the fact that the nonlinearly induced refractive index $\Delta n(x,z)=\int_{-\infty}^{\infty}R(x-\xi)|q(\xi,z)|^2d\xi$ depends only on the beam power, and is largely insensitive to the profile of the intensity [3,12].

Then we also change the power of the initial inputs arbitrarily, which are exemplified by $P_i=0.7P_9$ and $P_i=1.3P_9$. Alternatively, the initial inputs are $q(x,0)=\sqrt{0.7}r(x)$ and $q(x,0)=\sqrt{1.3}r(x)$, respectively. The evolutions are displayed in Figs. 2(a) and 2(b) of which are the contour plots of the amplitude for $P_i=0.7P_9$ and $P_i=1.3P_9$, respectively, the corresponding beam width are shown in Figs. 2(c) and 2(d). We can see that the evolutions in Fig. 2 appear exactly similar to those in Fig. 1, except that the average beam widths are changed. There is no significant difference in the standard deviation among the beam width in Figs. 2(c), 2(d) and 1(d).

Thirdly, we should consider the initial inputs with the beam width changed too, such as rescaling the $r(x)$ in the x direction. However, it is unnecessary in fact. Because the beam widths in Fig. 2 at a certain z_0 are varied from the initial beam width, and $q(x,z_0)$ can be also viewed as an initial input for the following evolution. That is to say, the cases

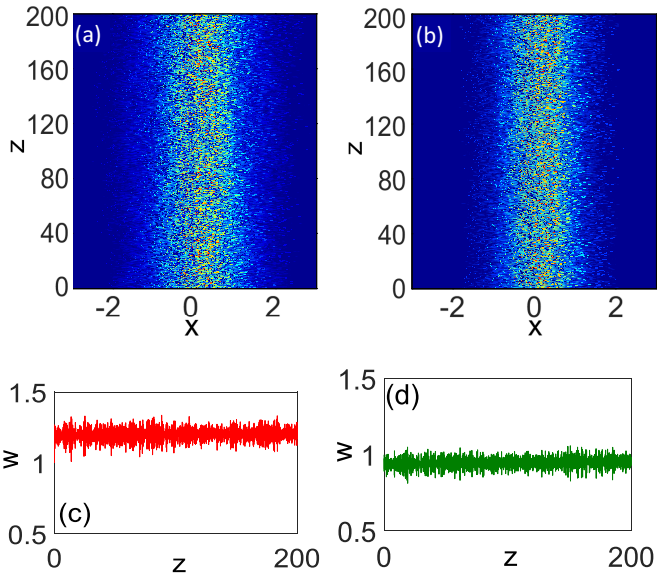

FIG. 2. The evolutions of random initial inputs with $P_i = 0.7P_9$ (left) and $P_i = 1.3P_9$ (right) in the ERF model. (a), (b)The contour plots of $|q(x, z)|$, (c), (d) the beam widths corresponding to (a), (b), respectively.

in Fig. 2 can represent the evolutions of absolutely random initial inputs. Then, about the model described by Eqs. (1) and (2) in a strong nonlocality, we can conclude that besides the high-order HGSS any random initial input (even with the beam width and power equal to those of the low-order HGSS) will evolve into a self-trapped beam with a nearly invariant beam width after a short transient process, while the initial inputs of the low-order HGSS evolve periodically or quasiperiodically [7,8]. Moreover, long enough simulations show that the power of the beam is conserved without any energy lost by radiation during the evolution.

For contrast, we also investigate the evolutions of random initial inputs in the phenomenological system with the GRF: $R(x) = 1/\sqrt{2\pi}\, w_m \exp(-x^2/2w_m^2)$. Similarly, three cases are considered: the initial inputs of the $r(x)$ profile [shown in Fig. 1(a)] with the input powers $P_i = P_9$, $P_i = 0.7P_9$, and $P_i = 1.3P_9$, respectively, in which P_9 is the nine-humped HGSS of Eq. (1) with the GRF. Interestingly, we find that all of them evolve periodically, as shown in Fig. 3. In order to demonstrate the periodicity clearly, a small region of evolution of $z \in [100, 105]$ are displayed. We give the contour plot of the amplitude only for the case of $P_i = P_9$ in Fig. 3(a), since the scenes for $P_i \neq P_9$ are completely similar. The evolutions of beam width are shown in Fig. 3(b) (for $P_i = P_9$) and 3(c) (the upper red solid curve for $P_i = 0.7P_9$, the lower green dashed curve for $P_i = 1.3P_9$), which show the periodicity more obviously. The distinction of the evolution in the above two systems may arise from the crucial difference of the two kinds of nonlinear response functions: the ERF in the real physical media is singular, while the unphysical GRF is nonsingular.

III. CHAOTIC PROPERTY WITH POSITIVE LYAPUNOV EXPONENTS AND SPATIAL DECOHERENCE

To confirm whether the evolution is chaotic or not, we first calculate the maximal Lyapunov exponents since a positive

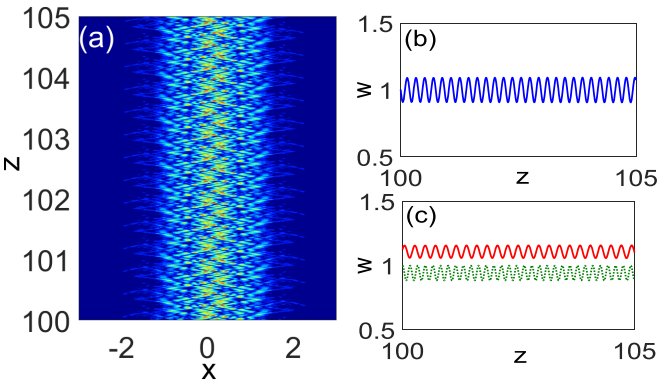

FIG. 3. The periodic evolutions of random initial inputs for the unphysical GRF model. (a) The contour plot of $|q(x, z)|$ for $P_i = P_9$, (b) the beam widths corresponding to (a). (c) The beam widths for $P_i = 0.7P_9$ (the upper red solid curve) and $P_i = 1.3P_9$ (the lower green dashed curve), respectively.

Lyapunov exponent is a signature of chaos [30–32]. The maximal Lyapunov exponent measures the typical exponential rate of growth of an infinitesimal perturbation, which can be computed by the so-called standard method: [30,33–36]

$$l = \lim_{\delta \to 0} \lim_{z \to \infty} \frac{1}{z} \ln \frac{d(q_1, q_2; z)}{d(q_1, q_2; 0)}, \tag{4}$$

where $d(q_1, q_2; z) = [\int_{-\infty}^{\infty} |q_1(x, z) - q_2(x, z)|^2 dx]^{1/2}$ is the distance (the L^2 norm in the Hilbert space) between two functions $q_1(x, z)$ and $q_2(x, z)$. The two initial values are $q_1(x, 0) = q(x, 0)$ and $q_2(x, 0) = q(x, 0) + \delta(x)$, where the initial perturbation $\delta(x)$ is assigned to be a random function with the amplitude as small as machine precision allows (e.g., in the order of 10^{-8}). Let $\lambda(z) = \lim_{\delta \to 0} \ln[d(q_1, q_2; z)/d(q_1, q_2; 0)]/z$, then $l = \lim_{z \to \infty} \lambda(z)$. That is to say, in a curve of λ versus z, the maximal Lyapunov exponent l is the convergent value of λ at a large enough z.

The maximal Lyapunov exponents of several cases mentioned above are shown in Fig. 4, in which the curves from top to bottom correspond to the evolutions of $P_i = 1.3P_9$ [Fig. 2(b)], $P_i = P_9$ [Fig. 1(b)], $P_i = 0.7P_9$ [Fig. 2(a)] in the ERF system and $P_i = P_9$ [Fig. 3(a)] in the GRF system, respectively. In the computation, we choose the window of the system $x \in [-30, 30]$, which is discretized into 4096

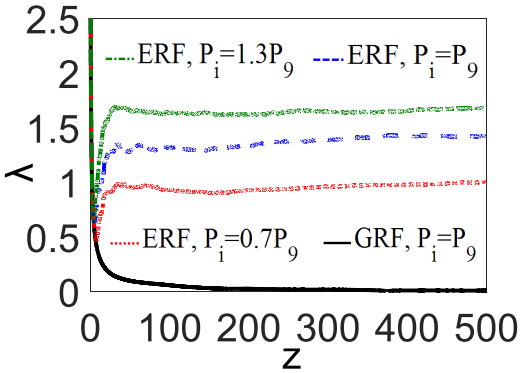

FIG. 4. The maximal Lyapunov exponents for several cases. The four curves from top to bottom are corresponding to the evolutions show in Fig. 2(b), Fig. 1(b), Fig. 2(a), and Fig. 3(a), respectively.

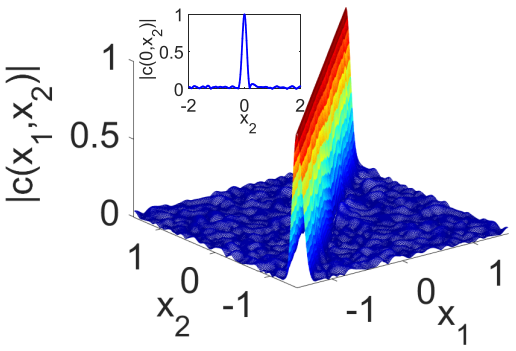

FIG. 5. The modulus of the spatial cross correlation function for the evolution of the random input $r(x)$.

points. We can see that the maximal Lyapunov exponent of the bottom curve is 0, which coincides with the periodic solution. The maximal Lyapunov exponents of the above three curves are all positive, about $l = 1.6, 1.4, 1.0$, respectively. As a matter of fact, for an infinite-dimensional system of partial differential equation, there exists theoretically a continuous spectrum of Lyapunov exponents, which should be the convergence of all the Lyapunov exponents calculated [35]. However, a positive maximal Lyapunov exponent is sufficient to indicate the chaotic behavior in the z direction. Also, we have testified that the maximal Lyapunov exponents show a good convergency (the relative error is less than 10%) by repeated calculation adopting different numbers of discretization points and other numerical parameters. Results suggest that the random input beam propagating in the strongly nonlocal nonlinear media with the ERF is chaotic.

Furthermore, we find that the values of $l\bar{w}^2$ are almost equal to each other for the three chaotic cases in Fig. 4, where the corresponding average beam widths are $\bar{w} \approx 0.94, 1.00, 1.19$ [shown in Fig. 2(d), Fig. 1(d), Fig. 2(c), respectively] from top to bottom. This means that the degree of nonlocality (denoted by $\bar{w}/w_m$) almost have no effect on the value of the maximal Lyapunov exponent in view of the scaling property of the nonlocal nonlinear Schrödinger equation and the maximal Lyapunov exponent [9,21,22]. By the way, it is worth mentioning that the value of the maximal Lyapunov exponent for an initial input with a different profile (even the equal beam width and power) may vary considerably.

In fact, for a partial differential system with respect to time and space, there are two kinds of chaotic states: the temporal chaos with spatial coherence (viewed as low-dimensional chaos) [37,38] and the spatiotemporal chaos with spatial decoherence [38]. In order to make clear the kind of our chaotic solutions, we will calculate the spatial cross correlation function of two long enough wave-amplitude series at locations x_1 and x_2

$$c(x_1, x_2) = \lim_{z_0 \to \infty} \frac{\int_0^{z_0} q(x_1, z) q^*(x_2, z) dz}{\sqrt{\int_0^{z_0} |q(x_1, z)|^2 dz \int_0^{z_0} |q(x_2, z)|^2 dz}}, \quad (5)$$

where the superscript $*$ denotes the conjugate complex. The modulus of c for the random input $r(x)$ are depicted in Fig. 5, from which we can see that $|c|$ equals 1 along the line $x_1 = x_2$ and decreases rapidly with the separation of two locations. The inset gives the cutting line of $|c(x_1, x_2)|$ at $x_1 = 0$ to show more clearly the rapid decline of $|c|$. The quick drop of correlation in the x direction means the spatial decoherence, which can be viewed as the indication of the chaotic behavior along the x direction [38–40]. So we can judge that the chaotic solutions are spatiotemporal chaos if z is viewed as time.

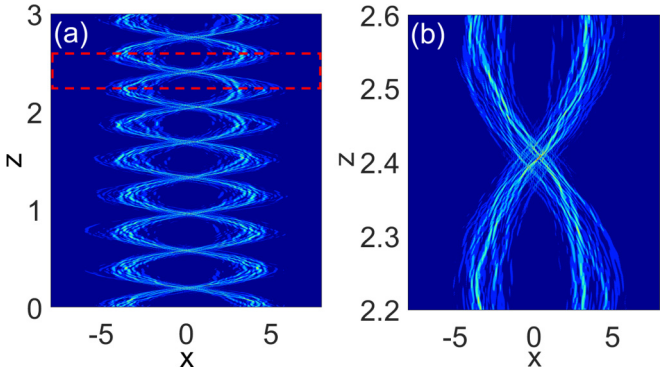

FIG. 6. The interaction of quasielastic collisions between the two identical beans shown in Fig. 1(b). (a) The contour plot of $|q(x, z)|$, (b) the partially enlarged detail of (a) in box.

IV. SOLITONLIKE PROPERTY WITH INTERACTION OF QUASIELASTIC COLLISIONS

In addition to the invariance of the beam width during the evolution, we find that the beams posses another typical property of an optical soliton: the particlelike interaction phenomena [6,14,41]. We explore the evolution of two identical random inputs $r(x)$'s, which are initially parallel and separated with a large enough distance [the center-to-center distance is $8w(0)$] to prevent the overlap of waves. The interaction of the two beams are displayed in Fig. 6. From Fig. 6(a) we can see that the two chaoticons attract each other and bend their trajectories, then combine and separate quasiperiodically. The scene is quite similar to the elastic collisions between two particles. The detail of a single collision is presented in Fig. 6(b), which is the enlargement of Fig. 6(a) in box. In fact, their interaction is of quasielastic collision, for it is actually accompanied by a small energy loss to radiation.

V. CONCLUSION

In summary, we demonstrate the general existence of chaoticons in the strongly nonlocal nonlinear media with the exponential-decay response by the evolution of the random initial inputs that have random initial transverse distributions and arbitrary input powers. The chaotic properties are presented by the positive maximal Lyapunov exponents and spatial decoherence, while the solitonlike properties are demonstrated by the invariance of beam width and the quasielastic particlelike interactions. Our findings may shine new light on the secret communication in the nonlocal nonlinear media.

ACKNOWLEDGMENTS

This research was supported by the National Natural Science Foundation of China, Grant No. 11704169. We are grateful to Professor Yuqi Li at East China Normal University for his helpful discussion.

[1] G. Assanto, *Nematicons: Spatial Optical Solitons in Nematic Liquid Crystals* (John Wiley & Sons, New Jersey, 2013).

[2] Q. Guo, D. Lu, and D. Deng, Nonlocal spatial optical solitons, in *Advances in Nonlinear Optics*, edited by X. Chen, Q. Guo, W. She, H. Zhang, and G. Zhang (De Gruyter, Berlin, 2015), pp. 227–305.

[3] A. W. Snyder and D. J. Mitchell, Accessible solitons, Science **276**, 1538 (1997).

[4] C. Conti, M. Peccianti, and G. Assanto, Route to Nonlocality and Observation of Accessible Solitons, Phys. Rev. Lett. **91**, 073901 (2003).

[5] C. Conti, M. Peccianti, and G. Assanto, Observation of Optical Spatial Solitons in a Highly Nonlocal Medium, Phys. Rev. Lett. **92**, 113902 (2004).

[6] W. Hu, T. Zhang, Q. Guo, L. Xuan, and S. Lan, Nonlocality-controlled interaction of spatial solitons in nematic liquid crystals, Appl. Phys. Lett. **89**, 071111 (2006).

[7] Z. Xu, Y. V. Kartashov, and L. Torner, Upper threshold for stability of multipole-mode solitons in nonlocal nonlinear media, Opt. Lett. **30**, 3171 (2005).

[8] L. Zhong, J. Yang, Z. Ren, and Q. Guo, Hermite-Gaussian stationary solutions in strongly nonlocal nonlinear optical media, Opt. Commun. **383**, 274 (2017).

[9] L. Zhong, Y. Li, Y. Chen, W. Hong, W. Hu, and Q. Guo, Chaoticons described by nonlocal nonlinear Schrödinger equation, Sci. Rep. **7**, 41438 (2017).

[10] Y. V. Izdebskaya, V. G. Shvedov, P. S. Jung, and W. Krolikowski, Stable vortex soliton in nonlocal media with orientational nonlinearity, Opt. Lett. **43**, 66 (2018).

[11] C. Rotschild, O. Cohen, O. Manela, and M. Segev, Solitons in Nonlinear Media with an Infinite Range of Nonlocality: First Observation of Coherent Elliptic Solitons and of Vortex-Ring Solitons, Phys. Rev. Lett. **95**, 213904 (2005).

[12] C. Rotschild, T. Schwartz, O. Cohen, and M. Segev, Incoherent spatial solitons in effectively instantaneous nonlinear media, Nat. Photon. **2**, 371 (2008).

[13] L. Dong and F. Ye, Stability of multipole-mode solitons in thermal nonlinear media, Phys. Rev. A **81**, 013815 (2010).

[14] C. Rotschild, B. Alfassi, O. Cohen, and M. Segev, Long-range interactions between optical solitons, Nat. Phys. **2**, 769 (2006).

[15] Q. Shou, Y. Liang, Q. Jiang, Y. Zheng, S. Lan, W. Hu, and Q. Guo, Boundary force exerted on spatial solitons in cylindrical strongly nonlocal media, Opt. Lett. **34**, 3523 (2009).

[16] Q. Shou, X. Zhang, W. Hu, and Q. Guo, Large phase shift of spatial solitons in lead glass, Opt. Lett. **36**, 4194 (2011).

[17] Q. Shou, D. Liu, X. Zhang, W. Hu, and Q. Guo, Large phase shift of spatial soliton in lead glass by cross-phase modulation in pump-signal geometry, Chin. Phys. B **23**, 084204 (2014).

[18] Q. Shou, M. Wu, and Q. Guo, Large phase shift of (1+1)-dimensional nonlocal spatial solitons in lead glass, Opt. Commun. **338**, 133 (2015).

[19] D. Buccoliero, A. S. Desyatnikov, W. Krolikowski, and Y. S. Kivshar, Laguerre and Hermite Soliton Clusters in Nonlocal Nonlinear Media, Phys. Rev. Lett. **98**, 053901 (2007).

[20] S. Skupin, O. Bang, D. Edmundson, and W. Krolikowski, Stability of two-dimensional spatial solitons in nonlocal nonlinear media, Phys. Rev. E **73**, 066603 (2006).

[21] S. Ouyang, Q. Guo, and W. Hu, Perturbative analysis of generally nonlocal spatial optical solitons, Phys. Rev. E **74**, 036622 (2006).

[22] G. Liang, W. Hong, and Q. Guo, Spatial solitons with complicated structure in nonlocal nonlinear media, Opt. Express **24**, 28784 (2016).

[23] Z. Wang, Q. Guo, W. Hong, and W. Hu, Modulational instability in nonlocal Kerr media with sine-oscillatory response, Opt. Commun. **394**, 31 (2017).

[24] Q. Guo, B. Luo, F. Yi, S. Chi, and Y. Xie, Large phase shift of nonlocal optical spatial solitons, Phys. Rev. E **69**, 016602 (2004).

[25] Y. Huang, Q. Guo, and J. Cao, Optical beams in lossy non-local Kerr media, Opt. Commun. **261**, 175 (2006).

[26] D. Deng, X. Zhao, Q. Guo, and S. Lan, Hermite-Gaussian breathers and solitons in strongly nonlocal nonlinear media, J. Opt. Soc. Am. B **24**, 2537 (2007).

[27] A. Picozzi and J. Garnier, Incoherent Soliton Turbulence in Nonlocal Nonlinear Media, Phys. Rev. Lett. **107**, 233901 (2011).

[28] N. Verschueren, U. Bortolozzo, M. G. Clerc, and S. Residori, Spatiotemporal Chaotic Localized State in Liquid Crystal Light Valve Experiments with Optical Feedback, Phys. Rev. Lett. **110**, 104101 (2013).

[29] N. Verschueren, U. Bortolozzo, M. G. Clerc, and S. Residori, Chaoticon: localized pattern with permanent dynamics, Phil. Trans. R. Soc. A **372**, 0011 (2014).

[30] J. C. Sprott, *Chaos and Time-Series Analysis* (Oxford University Press, Oxford, 2003).

[31] H. G. Schuster and W. Just, *Deterministic Chaos: An Introduction* (Wiley-VCH Verlag GmbH, Weinheim, 2005).

[32] J. J. Lissauer, Chaotic motion in the solar system, Rev. Mod. Phys. **71**, 835 (1999).

[33] A. C. Cassidy, D. Mason, V. Dunjko, and M. Olshanii, Threshold for Chaos and Thermalization in the One-Dimensional Mean-Field Bose-Hubbard Model, Phys. Rev. Lett. **102**, 025302 (2009).

[34] I. Brezinova, L. A. Collins, K. Ludwig, B. I. Schneider, and J. Burgdorfer, Wave chaos in the nonequilibrium dynamics of the Gross-Pitaevskii equation, Phys. Rev. A **83**, 043611 (2011).

[35] M. G. Clerc and N. Verschueren, Quasiperiodicity route to spatiotemporal chaos in one-dimensional pattern-forming systems, Phys. Rev. E **88**, 052916 (2013).

[36] G. Tancredi, A. Sánchez, and F. Roig, A comparison between methods to compute Lyapunov exponents, Astron. J. **121**, 1171 (2001).

[37] K. Nozaki and N. Bekki, Chaotic solitons in a plasma driven by an rf field, J. Phys. Soc. Jpn. **54**, 2363 (1985); K. Nozaki, and N. Bekki, Low-dimensional chaos in a driven damped nonlinear Schrödinger equation, Physica D **21**, 381 (1986).

[38] D. Cai and D. W. McLaughlin, Chaotic and turbulent behavior of unstable one-dimensional nonlinear dispersive waves, J. Math. Phys. **41**, 4125 (2000).

[39] Y. Zhang and J. J. Jiang, Spatiotemporal chaos in excised larynx vibrations, Phys. Rev. E **72**, 035201 (2005).

[40] R. Ramaswamy and F. Julicher, Activity induces traveling waves, vortices and spatiotemporal chaos in a model actomyosin layer, Sci. Rep. **6**, 20838 (2016).

[41] G. I. Stegeman and M. Segev, Optical spatial solitons and their interactions: university and diversity, Science **286**, 1518 (1999).